

WAC FILE COPY

4

AD-A195 891

TECHNICAL REPORT BRL-TR-3804

**WRL**

1988 - Serving the Army for Fifty Years - 1938

**PRESSURE-FLAMEFRONT CORRELATIONS  
IN THE SIMULATOR IGNITION STUDIES  
OF 105-MM TANK CHARGES**

DTIC

JUN 14 1988

LANG-MANN CHANG

MARCH 1988

APPROVED FOR PUBLIC RELEASE; DISTRIBUTION UNLIMITED.

U.S. ARMY LABORATORY COMMAND

**BALLISTICS RESEARCH LABORATORY**

ABERDEEN PROVING GROUND, MARYLAND

REPORT DOCUMENTATION PAGE

1a. REPORT SECURITY CLASSIFICATION <b>Unclassified</b>		1b. RESTRICTIVE MARKINGS	
2a. SECURITY CLASSIFICATION AUTHORITY		3. DISTRIBUTION / AVAILABILITY OF REPORT	
2b. DECLASSIFICATION / DOWNGRADING SCHEDULE			
4. PERFORMING ORGANIZATION REPORT NUMBER(S) Technical Report BRL TR-2891		5. MONITORING ORGANIZATION REPORT NUMBER(S)	
6a. NAME OF PERFORMING ORGANIZATION US Army Ballistic Research Laboratory	6b. OFFICE SYMBOL (if applicable) SLCBR-IB	7a. NAME OF MONITORING ORGANIZATION	
6c. ADDRESS (City, State, and ZIP Code) Aberdeen Proving Ground Maryland 21005-5066		7b. ADDRESS (City, State, and ZIP Code)	
8a. NAME OF FUNDING / SPONSORING ORGANIZATION	8b. OFFICE SYMBOL (if applicable)	9. PROCUREMENT INSTRUMENT IDENTIFICATION NUMBER	
8c. ADDRESS (City, State, and ZIP Code)		10. SOURCE OF FUNDING NUMBERS	
		PROGRAM ELEMENT NO.	PROJECT NO.
		TASK NO.	WORK UNIT ACCESSION NO.
11. TITLE (Include Security Classification) Pressure-Flamespread Correlations in Simulator Ignition Studies of 105-mm Tank Charges			
12. PERSONAL AUTHOR(S) Lang-Mann Chang			
13a. TYPE OF REPORT Technical Report	13b. TIME COVERED FROM 3/86 TO 10/86	14. DATE OF REPORT (Year, Month, Day)	15. PAGE COUNT 36
16. SUPPLEMENTARY NOTATION <i>Pressure flame spreading correlation; Propelling charges; LOVA propellant. (cdc)</i>			
17. COSATI CODES		18. SUBJECT TERMS (Continue on reverse if necessary and identify by block number)	
FIELD	GROUP	SUB-GROUP	
21	02		
19	10		
		Gun Simulator, Ignition Studies, Pressure-Flamespread Correlations, LOVA Propellant, Pressure Data, Flamespreading	
19. ABSTRACT (Continue on reverse if necessary and identify by block number) Ignition diagnostics via a transparent gun chamber simulator have become an integral part of efforts in the development of advanced tank gun charges at the US Army Ballistic Research Laboratory. The diagnostics provide insights into the ignition processes occurring during the early phase of the interior ballistic cycle. In the studies, the pressure and photographic data obtained are the most important in analyzing the functioning of the ignition system, the ignition of propelling charges, and the formation of pressure waves. In the present study, we have established close correlations between these two kinds of data. The correlations can help one better understand the physical phenomena, the pressure distribution and flamespreading in particular, occurring in the 105-mm tank gun chamber. Furthermore, the correlations can enable one to visualize the flamespreading by examining the pressure-time curves alone and vice versa in many cases. In addition, effective ignition of propellant is characterized and the effects of apparent ullage appearing in a cartridge on the early phase of the ignition processes are discussed. Keywords: Tank gun simulator.			
20. DISTRIBUTION / AVAILABILITY OF ABSTRACT <input checked="" type="checkbox"/> UNCLASSIFIED / UNLIMITED <input checked="" type="checkbox"/> SAME AS RPT. <input type="checkbox"/> DTIC USERS		21. ABSTRACT SECURITY CLASSIFICATION Unclassified	
22a. NAME OF RESPONSIBLE INDIVIDUAL Lang-Mann Chang		22b. TELEPHONE (Include Area Code) (301) 278-6107	22c. OFFICE SYMBOL SLCBR-IB-P

TABLE OF CONTENTS

	Page
LIST OF FIGURES.....	5
LIST OF TABLES.....	7
I. INTRODUCTION.....	9
II. EXPERIMENTAL APPARATUS.....	9
III. RESULTS AND DISCUSSION.....	10
A. Time Sequence of Occurrence of Pressure Peaks.....	11
1. $P_{1p}$ Occurs Before $P_{3p}$ ( $t_{1p} < t_{3p}$ ).....	12
2. $P_{1p}$ Occurs After $P_{3p}$ ( $t_{1p} > t_{3p}$ ).....	15
3. $P_{1p}$ and $P_{3p}$ Occur at Approximately the Same Time ( $t_{1p} \approx t_{3p}$ ).....	16
B. Pressure Difference Between Breech and Projectile at the Instant That the Chamber Ruptures.....	18
C. Pressure Difference Between Breech and Projectile Prior to Chamber Rupture.....	19
D. Ignition Delay, $t_{ig}$ .....	20
E. Effective Ignition of a Propelling Charge.....	25
F. Ullage Effects.....	25
IV. SUMMARY AND CONCLUSIONS.....	28
REFERENCES.....	30
DISTRIBUTION LIST.....	31



Accession For	
NTIS CRA&I	<input checked="" type="checkbox"/>
DTIC TAB	<input type="checkbox"/>
Unannounced	<input type="checkbox"/>
Justification	
By _____	
Distribution/	
Availability Codes	
Dist	Availability/ or restricted
A-1	

## LIST OF FIGURES

Figure		Page
1	Cross-Section View of the 105-mm Gun Simulator.....	10
2	Experimental Arrangement.....	11
3	Pressure Rise and Flame spreading, $t_{1p} < t_{3p}$ .....	13
4	Pressure Rise and Flamespreading, $t_{1p} < t_{3p}$ .....	14
5	Pressure Rise and Flamespreading, $t_{1p} > t_{3p}$ .....	15
6	Pressure Rise and Flamespreading, $t_{1p} > t_{3p}$ .....	16
7	Pressure Rise and Flamespreading, $t_{1p} \approx t_{3p}$ and Large $dP_r$ .....	17
8	Pressure Rise and Flamespreading, $t_{1p} \approx t_{3p}$ and Small $dP_r$ .....	17
9	Pressure Rise and Flamespreading, Small $dP_r$ (referring to Figures 7a and 8a).....	19
10	Pressure Difference Between Breech and Projectile.....	20
11	Flame Front Travel Along Chamber Length.....	21
12	Comparison of Pressure Differences, $dP$ , Resulting From Gun Firing.....	21
13	Pressure Rise and Flamespreading, Large $t_{ig}$ .....	23
14	Pressure Rise and Flamespreading, Small $t_{ig}$ .....	23
15	Primers.....	24
16	Flame Front Travel Along Chamber Length.....	24
17	Comparison of Ignition Delays, $t_{ig}$ , Resulting From Gun Firings.....	25
18	Configurations of Ullage in Propellant Packed Chamber.....	26
19	Pressure Rise and Flamespreading in Chambers With Ullage (corresponding to the configuration shown in Figure 18a).....	27

LIST OF TABLES

Table	Page
1 Pressure-Time Data.....	12
2 Ballistic Performance in Gun Firing.....	22

## I. INTRODUCTION

In recent years, simulator diagnostics have become an important procedure in support of the development of advanced large caliber gun ammunition at the U.S. Army Ballistic Research Laboratory (SRL).<sup>1-4</sup> Particularly, in the LOVA technology development program the diagnostic procedure has been extensively used for the performance evaluation of various LOVA formulations as well as the novel ignition systems tailored for LOVA propelling charges. This diagnostic technique also has been a very useful tool for unveiling the causes of high amplitude pressure waves occurring in gun firings.<sup>5</sup>

The simulator employed was fabricated from a transparent acrylic tube which offered excellent visualization of the events occurring inside. Pressure rises at the breech and forward ends of the simulator chamber were measured by using quartz PCB pressure gages.

Via simulator diagnostics many ignition phenomena occurring during the early phase of the ballistic cycle can be observed and analyzed. These phenomena include the functioning of the ignition system, flamespreading, formation of pressure waves, and propellant bed motion and compaction.

Of the data recorded in the diagnostics, the pressure histories at the breech and forward ends of the simulator chamber and the flamespreading along the propellant bed are most important. In general, both data should be examined for the best understanding of the ignition phenomena. However, with the correlations we established between these two kinds of data, it is possible to visualize flamespreading fairly accurately by examining the pressure-time curves alone. The vice versa is true in many cases. Thus the correlations are useful in the situation that only one kind of the data is

---

<sup>1</sup>T.C. Minor, "Ignition Phenomena in Combustible-cased Stick Propellant Charge," 19th JANNAF Combustion Meeting, CPIA Publication 366, Vol. I, pp. 555-567, Oct 1982.

<sup>2</sup>T.C. Minor, "Experimental Studies of Multidimensional Two-phase Flow Processes in Interior Ballistics," ARBRL-MR-03248, U.S. Army Ballistic Research Laboratory, Apr 1983 (AD A128034)

<sup>3</sup>L.M. Chang and J.J. Rocchio, "Early Phase Interior Ballistic Cycle Studies in a Tank Gun Simulator," proceeding of the 8th International Symposium on Ballistics, pp. I-13 - I-24, Oct 1984.

<sup>4</sup>L.M. Chang, "Early Phase Ignition Phenomena Observed in a Tank Gun Chamber," 21st JANNAF Combustion Meeting, CPIA Publication 412, Vol. II, pp. 301-311, Oct 1984.

<sup>5</sup>L.M. Chang, "Mechanism of Formation of High Amplitude Pressure Waves in the 5-In./54 LOVA Propelling Charge," 23rd JANNAF Combustion Meeting, CPIA Publication 457, Vol. II, pp. 297-306, Oct 1986.

available as well as to help one to better understand the ignition processes. This report is principally to present such correlations established based on the data obtained in various simulator diagnostics programs involved in the development of the advanced LOVA charges for the 105-mm tank gun system. In addition, effects of apparent ullage appearing in a cartridge are analyzed.

## II. EXPERIMENTAL APPARATUS

Figure 1 presents a cross-sectional view of the 105-mm tank gun simulator. The chamber of the simulator was made from a transparent cast acrylic tubing with inside and outside diameters of 127 mm and 152 mm, respectively. It offers excellent visualization for the recording of the events occurring inside. The chamber was capable of withstanding dynamic pressures in excess of 21 MPa (3000 psi) before rupturing. The rear end of the chamber was adapted to the base of a real cartridge and its forward end to a short gun barrel in which an inert projectile was loaded. The simulator thus resembled the configuration in the 105-mm gun system. The unit was mounted on a steel fixture.

Figure 2 illustrates the experimental arrangement for the simulator diagnostics. The instrumentation used included three pressure gages, two Hycam 40 high-speed 16-mm cameras, one X-ray head, and one linear position transducer. The pressure gages (quartz PCB Model 113A23) monitored the pressure histories at the two ends of the chamber. As indicated in Figure 1,  $P_1$  and  $P_2$  gages were installed in the breech and  $P_3$  gage in the projectile afterbody near the forward end of the chamber. Camera A and Camera B, located  $90^\circ$  apart, allowed simultaneous recording of the flamespreading along the chamber length from two different angles. The framing rate of the cameras was set at 5000 pictures per second. The X-ray head was positioned on one side of the chamber and a cassette containing a Kodak XR-5 film on the opposite side to record the propellant bed motion and compaction. The linear position transducer (Schaevitz Linear Variable Differential Transformer) was attached to the projectile nose for recording the projectile motion as a function of time. The entire fire control, data acquisition, and data reduction were performed by using the Ballistic Data Acquisition System (BALDAS) at the BRL.

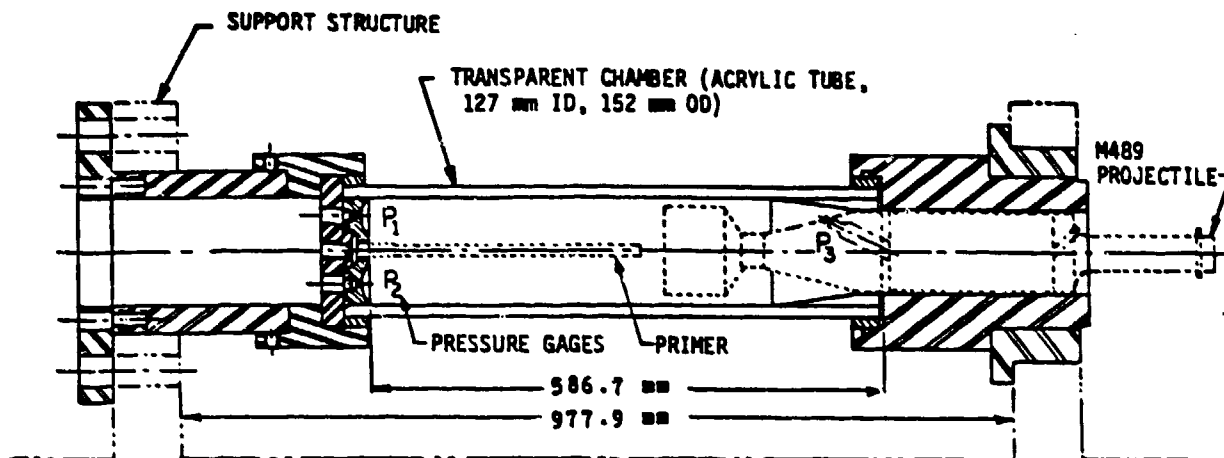


Figure 1. Cross-Sectional View of the 105-mm Gun Simulator

All of the simulator chambers, except indicated otherwise, were fully packed with propellant without apparent ullage. The packing procedure consisted of allowing the propellant to freely fall into the chamber which was standing vertically. This ensured good reproducibility of propellant packing density.

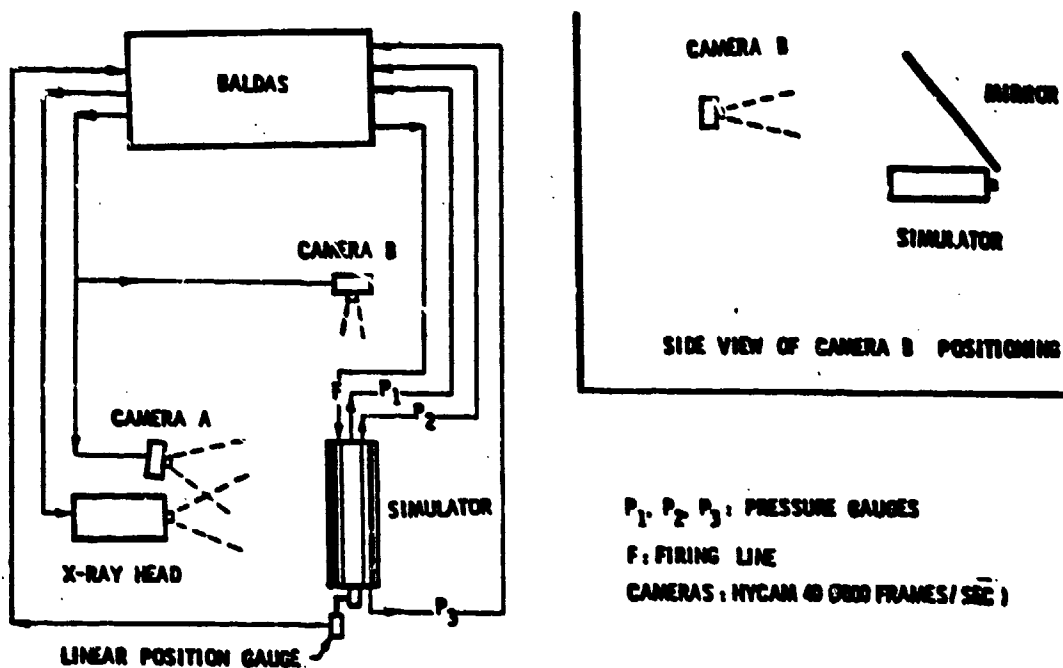


Figure 2. Experimental Arrangement

### III. RESULTS AND DISCUSSION

The following will present the correlations between the pressure data and the flamespreading in the propellant bed obtained via the diagnostics. The correlations are established according to:

- o the time sequence of the occurrence of the pressure peaks at the breech and at the projectile
- o the pressure difference between the breech and the projectile at the instant that the chamber ruptured
- o the pressure difference of the two pressures prior to the chamber rupture
- o the ignition delay of the propellant

The results are also correlated with the data from gun firing tests when such data are available. In addition, effects of apparent ullage on the initial pressure rise and flamespreading are analyzed.

## A. Time Sequence of Occurrence of Pressure Peaks

All of the acrylic chambers used in this study were supplied by the same manufacturer. They were uniform in structure and free from visible defects or scratches. It can be reasonably assumed that all chambers had approximate the same strength and in each chamber the chamber wall had a uniform strength along its length.

In the following,  $P_1$  and  $P_2$  denote the pressures recorded by the two gauges installed in the breach, while  $P_3$  in the projectile afterbody near the forward end of the chamber, as indicated in Figure 1. The peak values of the three pressures are designated as  $P_{1p}$ ,  $P_{2p}$ , and  $P_{3p}$ , respectively. They occurred immediately following the rupture of the chamber. Examination of the photographic data recorded on the high-speed film reveals that the first pressure peak of the three curves took place within 0.2 ms after the initiation of the the chamber rupture. Furthermore, let the instant at which  $P_{1p}$  occurred be denoted by  $t_{1p}$ ,  $P_{2p}$  by  $t_{2p}$ , and  $P_{3p}$  by  $t_{3p}$ . Here the times refer to the times after application of the firing voltage. Comparison of pressure measurements shows no significant discrepancy between  $P_1$  and  $P_2$  curves in each round when the round was fully packed without ullage. Thus we hereafter treat  $P_2$  the same as  $P_1$ . There are three possible orders of the occurrence of  $P_{1p}$  relative to the occurrence of  $P_{3p}$ : before (i.e.,  $t_{1p} < t_{3p}$ ), after (i.e.,  $t_{1p} > t_{3p}$ ), or at about the same time (i.e.,  $t_{1p} \approx t_{3p}$ ). For the convenience of the following analysis, we define a time difference as  $dt_p = t_{3p} - t_{1p}$ .

### 1. $P_{1p}$ Occurs Before $P_{3p}$ ( $t_{1p} < t_{3p}$ )

Figures 3a and 4a present typical pressure-time curves of two rounds in this category. In the figures the breach peak pressure,  $P_{1p}$ , occurred prior to the projectile peak pressure,  $P_{3p}$ , by time intervals of  $dt_p = 0.23$  ms and  $dt_p = 0.3$  ms, respectively. Values of  $dt_p$  and other related data directly measured from the corresponding pressure-time curves are listed in Table 1. Based on the pressure and photographic data gathered from the tests with the

Table 1. Pressure-Time Data

<u>ROUND</u> (prop./pri. body/ igniter mat.)	$t_{1p}$ (ms)	$t_{3p}$ (ms)	$dt_p$ (ms)	$P_{1p}$ (MPa)	$P_{3p}$ (MPa)	R
M30/M83/Benite	8.74	8.97	0.23	18.00	7.36	.810
LOVA A2-101/M83/Benite	18.10	18.10	0.00	23.80	12.70	.230
LOVA A2-102/M83/Benite	24.30	24.60	0.30	13.40	9.70	.610
LOVA A2-101/E-tip/Benite	22.80	22.90	-0.10	23.50	21.70	0.005
LOVA 1289BL/M83/6828	7.30	7.03	-0.27	22.11	30.56	-0.690
LOVA 1289BL/M83/Benite	13.68	13.56	-0.12	24.00	22.43	-0.010
LOVA 1289BL/EEF/6828	4.89	4.71	-0.18	23.50	22.24	-0.090
LOVA 1289BL/EEF/6856	9.53	9.34	-0.19	20.63	18.00	-0.020
LOVA 1289BL/EEF/M9+5ZAL	6.25	6.55	-0.30	22.89	25.76	-0.300

EEF body: 39 holes (3.175 mm in diameter) in body and 4 holes (3.1/5 mm in diameter) in vented tip.

105-mm tank gun simulator, we can practically establish a criterion that  $dt_p$  is large when  $|dt_p| > 0.2$  ms, moderate when  $0.15$  ms  $< |dt_p| < 0.2$  ms, and small when  $|dt_p| < 0.15$  ms, where  $| |$  denotes an absolute value. The two  $dt_p$  values given above are considered large according to this criterion. A large positive value of  $dt_p$  means that the chamber rupture initiated very close to the breech. Meanwhile, if the pressure difference,  $dP = P_1 - P_3$ , at the instant of the rupture is also large, like the ones shown in Figures 3a and 4a, then the implication is that the chamber rupture initiated in a narrow

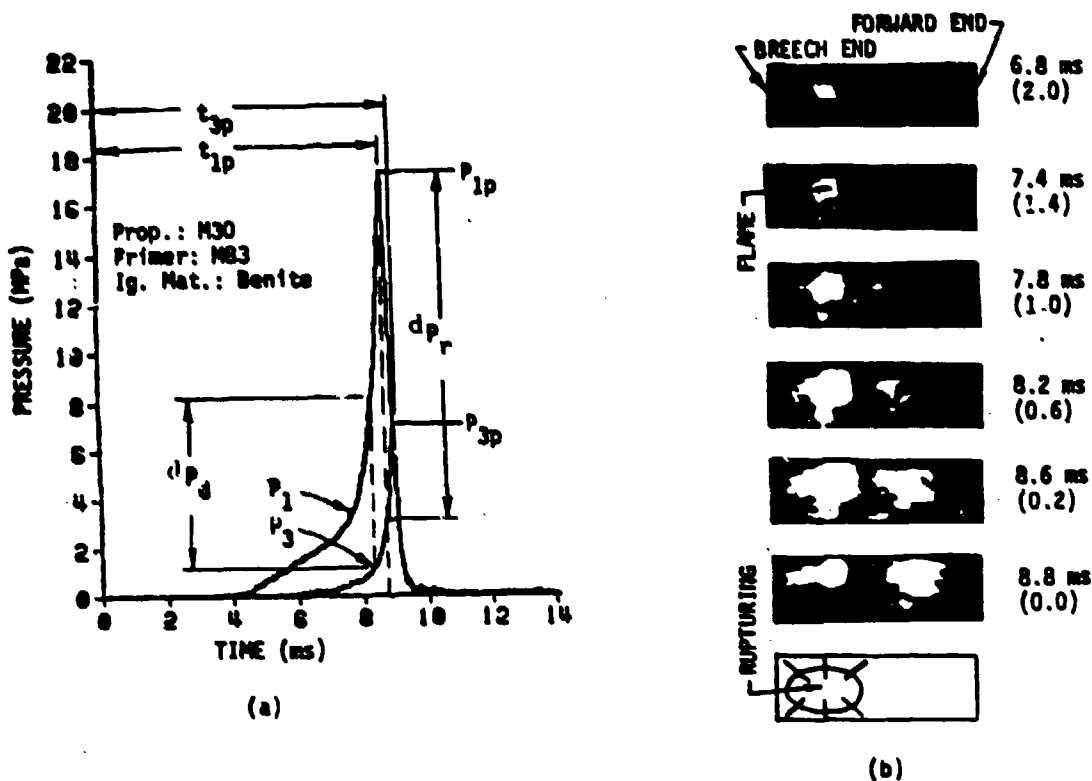


Figure 3. Pressure Rise and Flamespreading,  $t_{1p} < t_{3p}$

- Note: a. In all of the figures shown in this report the times indicated refer to the times after application of the firing voltage and the times in parentheses refer to the times before the instant of the chamber rupture.
- b. The pressure peak occurred within 0.2 ms after the initiation of the chamber rupture observed on the high-speed film.

section of the chamber near the breech. In other words, a high-pressure region existed near the breech and the pressure was highly localized. The role of the pressure difference,  $dP$ , will be further discussed later.

We then seek the correlation between the pressure-time curves and the photographic data. Figures 3b and 4b exhibit the flamespreading reprinted from the high-speed films corresponding to Figures 3a and 4a, respectively. The time indicated beside each frame in the figures is the time after application of the firing voltage. The times in the parentheses refer to the times before the instant of the chamber rupture. The films show that the ignition of the propellant started at approximately one quarter of the chamber length from the breech end, corresponding to the mid-section of the bayonet-type M83 primer used in the two rounds. The flame then advanced toward the two ends of the chamber. Before it had reached the forward end of the chamber, rupturing occurred near the breech end. The implication is that at the time of rupturing the pressure rise near the breech was much higher than that at the forward end and it had exceeded the strength limit of the chamber wall. This observation is fully concurrent with the implication of the pressure data stated earlier.

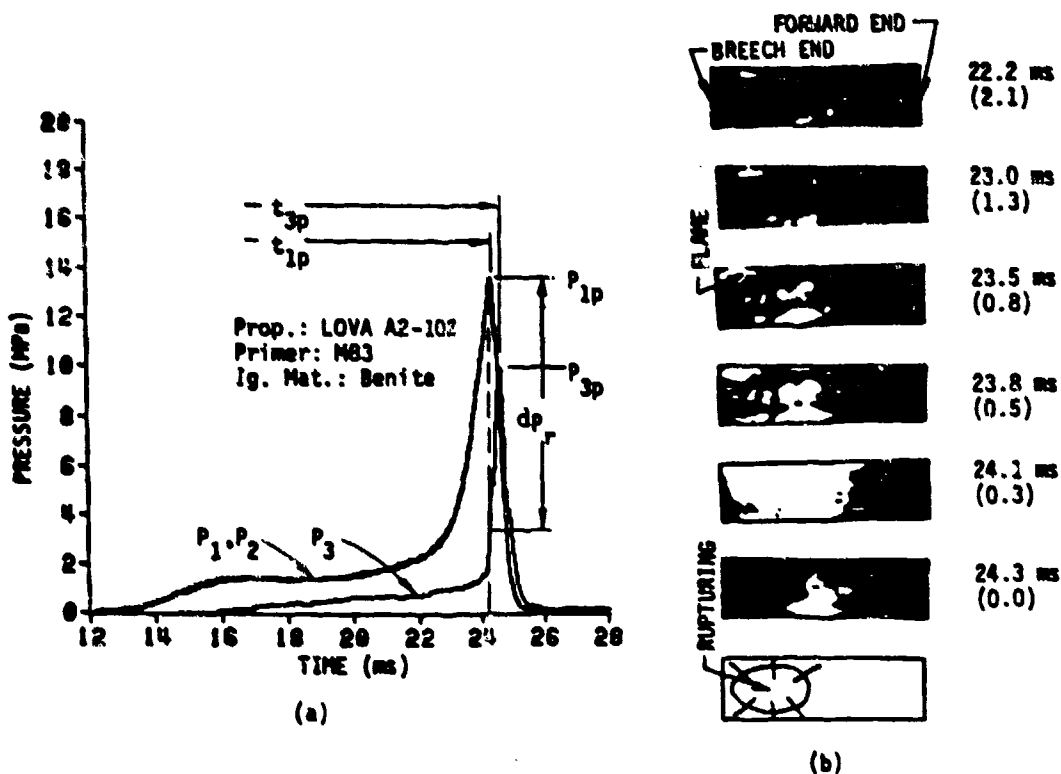


Figure 4. Pressure Rise and Flamespreading,  $t_{1p} < t_{3p}$

## 2. $P_{1p}$ Occurs After $P_{3p}$ ( $t_{1p} > t_{3p}$ )

In many cases, the breech pressure peak occurred after the projectile pressure peak and thus  $dt_p$  is negative. Figures 5a and 6a present two examples of this kind. After ignition, the projectile pressure,  $P_3$ , rose faster than the breech pressure,  $P_1$ , and eventually the  $P_3$  curve crossed over the  $P_1$  curve. Finally, the local pressure at or close to the gage  $P_3$  exceeded the strength limit of the chamber wall earlier than elsewhere along the chamber. Chamber rupture thus initiated at/or near the forward end of the chamber. This resulted in the occurrence of  $P_{3p}$  prior to  $P_{1p}$ . The magnitude of the negative  $dt_p$  can serve as a measurement of how close to the gage  $P_3$  the rupture initiated. From Table 1,  $dt_p = -0.3$  ms and  $dt_p = -0.44$  ms, respectively, for the two rounds shown in Figures 5a and 6a. These values are also considered large according to the above criterion. We then conclude that the chamber rupture initiated in a region very close to its forward end.

The photographic data corresponding to Figures 5a and 6a are presented in Figures 5b and 6b, respectively. From the data we see that the flame had covered the entire chamber length before the rupture occurred. The last frames of the photographic data show the location where the rupture initiated as seen on the films. The locations are in agreement with those interpreted using the pressure-time curves.

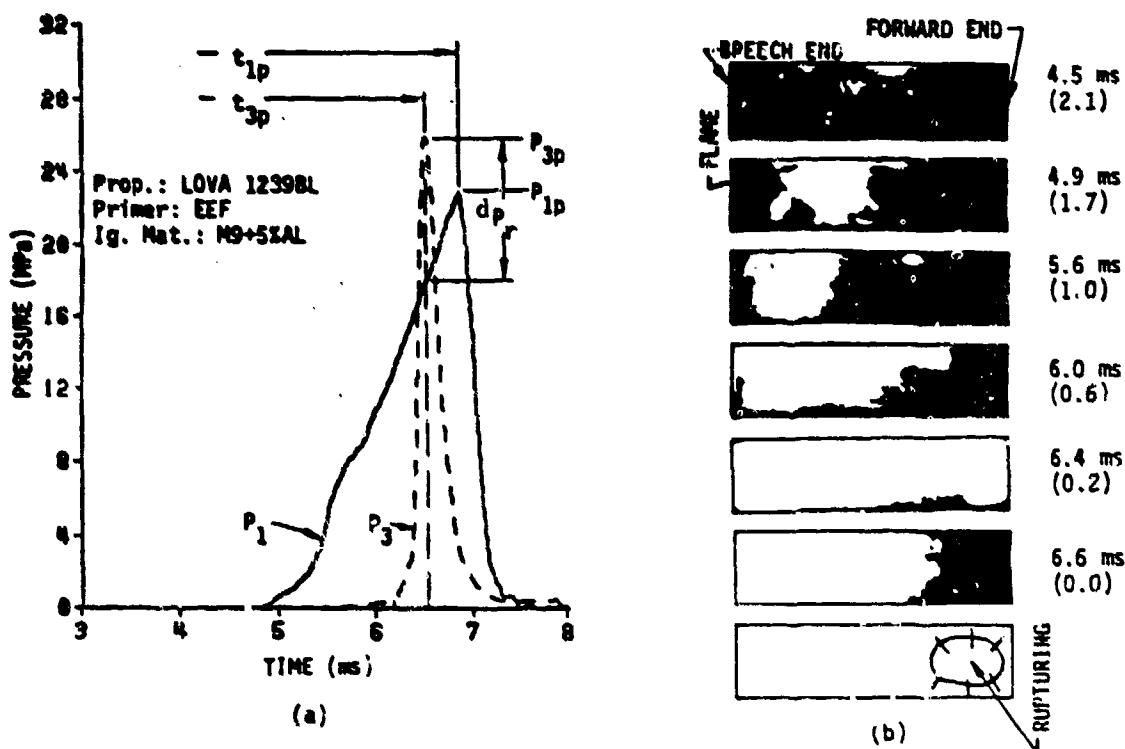


Figure 5. Pressure Rise and Flamespreading,  $t_{1p} > t_{3p}$

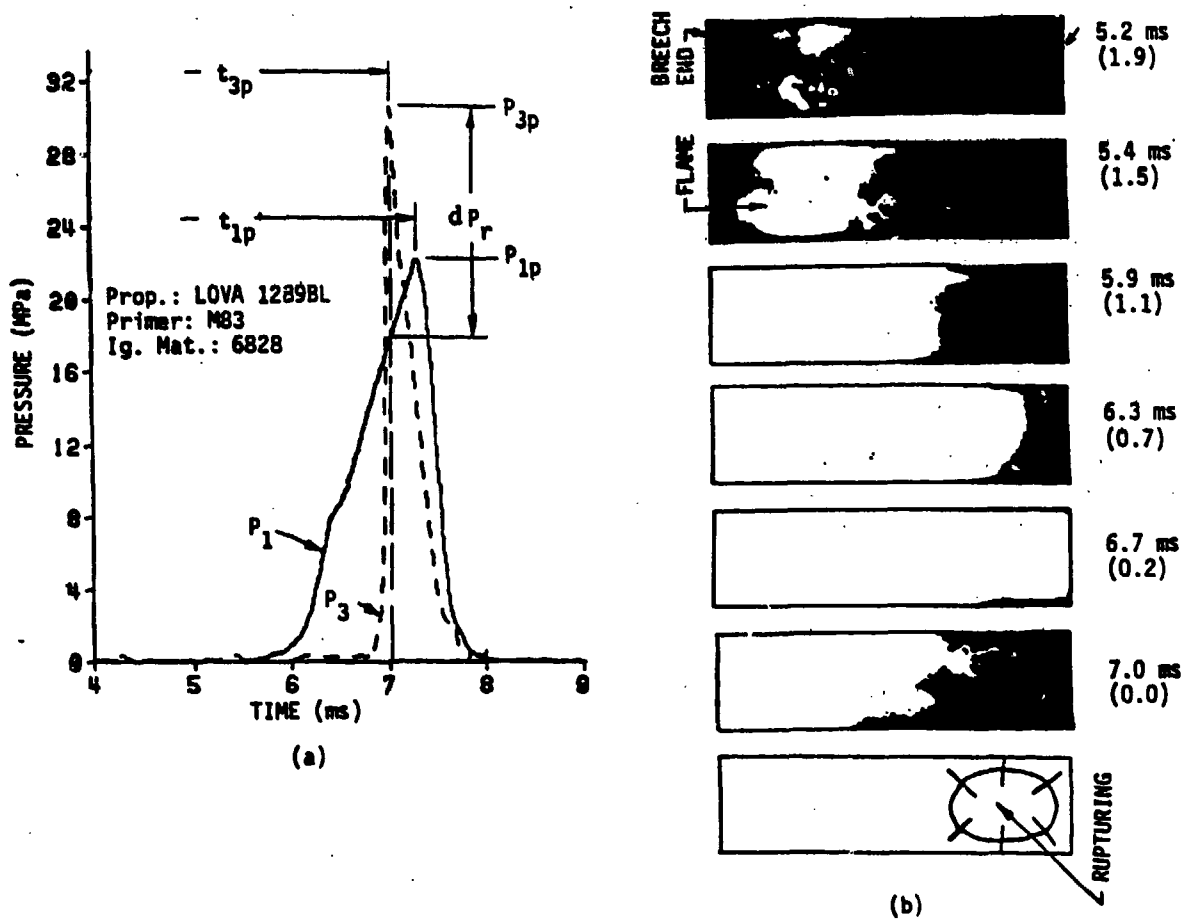


Figure 6. Pressure Rise and Flamespreading,  $t_{1p} > t_{3p}$

### 3. $P_{1p}$ and $P_{3p}$ Occurs at Approximately the Same Time ( $t_{1p} \approx t_{3p}$ )

As the third possible order of the occurrence of  $P_{1p}$  relative to  $P_{3p}$ , both pressure peaks may occur at about the same time, for which  $dt_p$  is small. Figures 7a and 8a exhibit the pressure-time curves belonging to this category. From Table 1,  $dt_p = 0$  and  $dt_p = -0.1$  ms for the two rounds, respectively. A small magnitude of  $dt_p$  can pose two implications: rupture occurring near the mid-section of the chamber or occurring uniformly over the entire chamber length. In the first case, the rupture resulted from a localized pressurization in the mid-section. The pressure peaks  $P_{1p}$  and  $P_{3p}$  would arrive at about the same time because of about equal distance to the gages  $P_1$  and  $P_3$ . In the second case, the chamber is pressurized fairly uniformly along the chamber length. The two pressure peaks would also arrive at about the same time. Thus to correctly interpret a small magnitude of  $dt_p$  we have to examine the pressure difference between  $P_1$  and  $P_3$  also. This will be detailed in Section B.

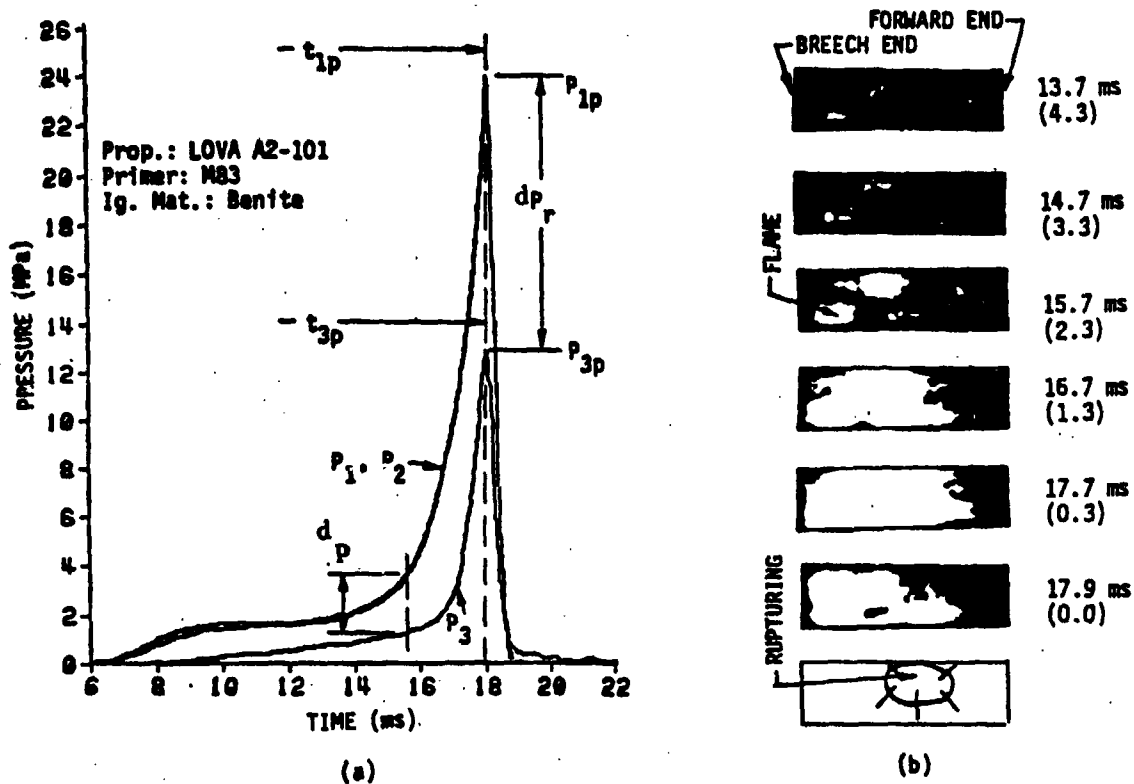


Figure 7. Pressure Rise and Flamespreading,  $t_{1p} \approx t_{3p}$  and Large  $dP_r$

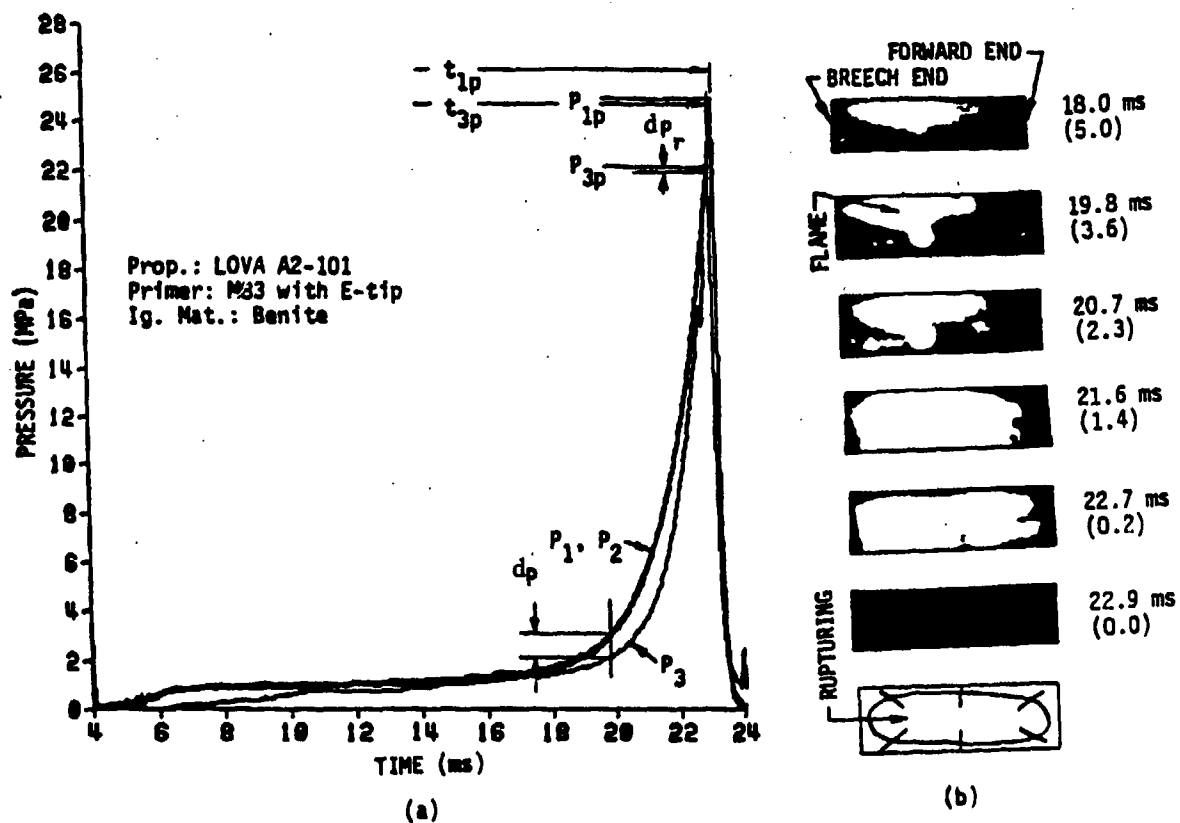


Figure 8. Pressure Rise and Flamespreading,  $t_{1p} \approx t_{3p}$  and Small  $dP_r$

The flamespreading corresponding to Figure 7a which belongs to the first case is presented in Figure 7b. The last frame in the figure shows that the chamber rupture initiated in a small region in the mid-section of the chamber. Corresponding to Figure 8a which belongs to the second case, the last frame in Figure 8b indicates that the chamber ruptured simultaneously over the entire chamber length. Again, the flamespreading observed is in agreement with the implication of the pressure data.

#### B. Pressure Difference Between Breech and Projectile at the Instant That the Chamber Ruptures

In general, the magnitude of the pressure difference between  $P_1$  and  $P_3$  can serve as a good indication of the uniformity of the pressurization in the propellant bed. For convenience, we define a ratio:

$$R = \frac{dP_r}{P_{1p}}$$

where  $dP_r$  is the pressure difference between  $P_1$  and  $P_3$ , both measured at the time that the first pressure peak occurred (i.e., it could be the time at which  $P_{1p}$  occurred or the time at which  $P_{3p}$  occurred, whichever occurred first). If  $P_{1p}$  occurs first,  $R > 0$ ; otherwise  $R < 0$ . When  $R$  is large (i.e.,  $|R| > 0.15$  based on our test results), the implication is that the pressurization and therefore the initiation of the chamber rupture are highly localized. The data shown in Figures 3a through 7a belong to this category. On the other hand, when  $R$  is small (i.e.,  $|R| < 0.1$ ) the implication is that the pressurization and therefore the initiation of the chamber rupture is fairly uniform along the chamber length. Figures 8a and 9a are examples of this kind. Such interpretations are applicable to all cases of  $dt_p > 0$ ,  $dt_p \approx 0$ , and  $dt_p < 0$ .

Now let us re-examine the statement made earlier that when  $dt_p$  is small, there are two possible implications: the rupture initiated in the mid-section or uniformly along the chamber. With the pressure difference accounted for, a correct interpretation can be ensured. Figure 7a shows the case that  $dt_p$  is small but  $R$  is large ( $R = 0.23$ , see Table 1). Therefore the rupture initiated locally in the mid-section of the chamber, as was confirmed by the photographic data shown in Figure 7b. Figure 8a shows the other case that both  $dt_p$  ( $= -0.1$  ms) and  $R$  ( $= 0.005$ ) are small. Therefore the rupture initiated uniformly along the chamber as shown in Figure 8b.

Next, let us examine two other cases as occurred in Figure 5a and 9a. In Figure 5a, both  $dt_p$  ( $= -0.3$  ms) and  $R$  ( $= -0.3$ ) are large in their absolute values. The implication is that the initiation of the chamber rupture was highly localized near the forward end of the chamber, as confirmed in Figure 5b. In Figure 9a,  $dt_p$  ( $= -0.19$  ms) is moderate, but  $R$  ( $= 0.02$ ) is small. The implication is that the rupture initiated somewhere near the forward end (since  $dt_p < 0$ ), however, the rupture of the other part of the chamber followed almost simultaneously (since  $R$  is small), as evidenced in Figure 9b.

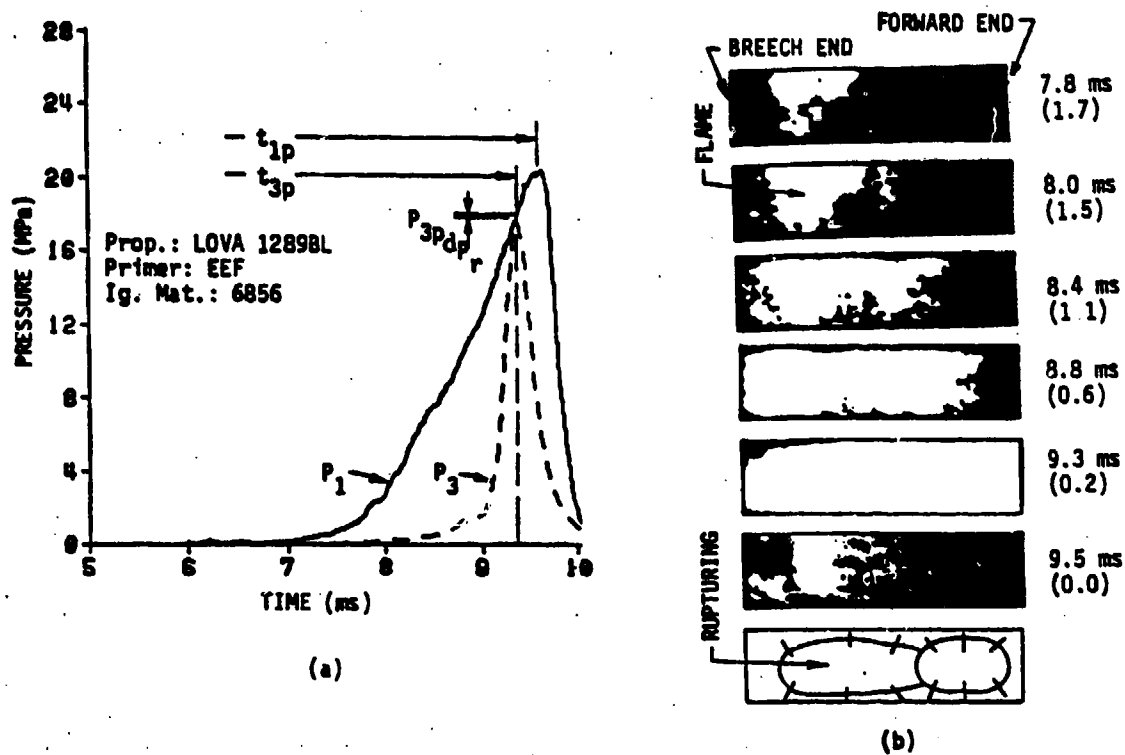


Figure 9. Pressure Rise and Flamespreading, Small  $dP_T$

### C. Pressure Difference Between Breech and Projectile Prior to Chamber Rupture

Due to the fact that the vented section of the M83 primer tube ranges from 80 mm to 290 mm from the breech end out of the total chamber length of 560 mm, the ignition of the propellant always initiates somewhere in the first half section of the chamber from the breech end. As a result, the pressure rise  $P_3$  at the projectile always lags behind the breech pressure rise  $P_1$  in the early stage of ignition process. The difference between them,  $P_d = P_1 - P_3$ , then can serve as a measurement of uniformity of chamber pressure. A small  $P_d$  implies uniform pressurization.

Figures 7a and 8a display data for two rounds, one with a large  $P_d$  and the other with a small  $P_d$ . Both rounds were packed with the same unimodal CAB/NC/RDX Lot A2-101 LOVA propellant and were ignited by the same igniter material, benite, but with primers in different body configurations. One used the standard M83 primer and the other used a modified M83 primer which was constructed by adding a 4-hole (4.064 mm in diameter) vented tip, called E-tip, to the primer tube. A comparison in Figure 10 shows that the round fired with E-tip primer resulted in a much smaller  $P_d$ . A correlation between  $P_d$  and flamespreading can be realized by observing Figures 7a and 8a together with Figures 7b and 8b. The flamespreading shown in Figure 7b was recorded in the round fired with the M83 primer. By the time of rupturing, which initiated near the breech, the flame had covered 90 percent of the propellant bed length. In Figure 8b, the flame in the round with the E-tip primer

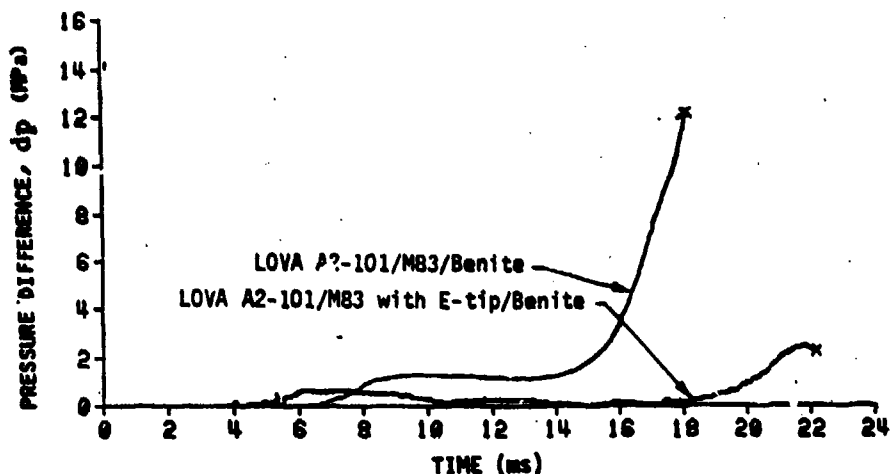


Figure 10. Pressure Difference Between Breech and Projectile

covered almost the entire propellant bed and the chamber ruptured simultaneously along its length. Furthermore, a direct comparison of the movements of flame fronts as a function of time is given in Figure 11. It is clear that the round with the E-tip primer had better flamespreading. The results are in concurrence with those interpreted from the pressure curves shown in Figures 7a and 8a.

Figure 12 presents the gun firing test data for two three-round groups using the M83 primer and the E-tip primer, respectively. We see that the data on the right hand side for the E-tip primer show a smaller pressure difference  $dp$ , which implies a more uniform chamber pressure distribution. This results in an improvement in ballistic performance in terms of the standard deviations of breech pressures, muzzle velocities, and temperature coefficients for the rounds using the E-tip primer as compared in Table 2.

#### D. Ignition Delay, $t_{ig}$

Although there is no unique way to define the ignition delay of propellant, the implication is clear that it is an indication of how quickly propellant is ignited and starts massive burning. In this study, for the convenience of comparison, we define the ignition delay as  $t_{ig} = t_i - t_a$  where  $t_i$  is the instant at which the recorded pressure starts to rise and  $t_a$  the instant at which the pressure reaches 2 MPa, as indicated in Figures 13a and 14a. The ignition delay, in general, is a function of several variables such as temperature, type of propellant (composition, grain geometry, particle size, etc.), body configuration of primer, and igniter material. A long ignition delay may be associated with the variability of interior ballistic performance. Thus it is an important factor to be considered in the performance evaluation of a new primer.

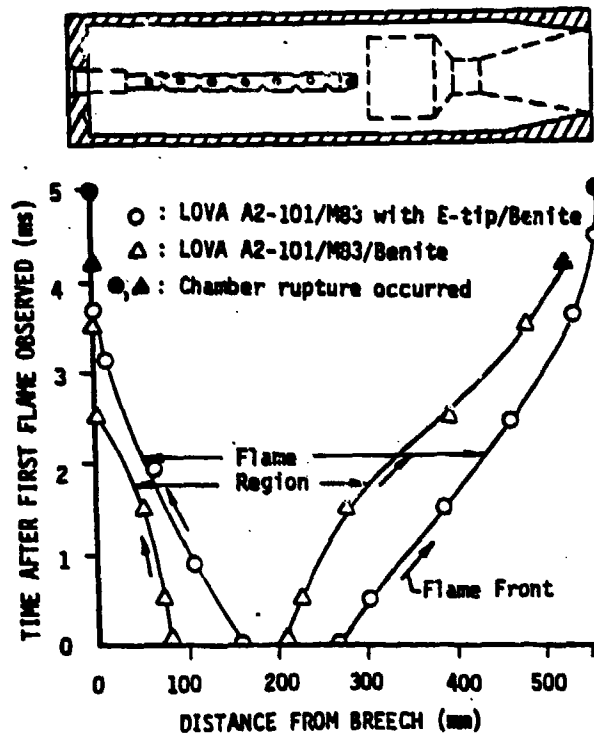


Figure 11. Flame Front Travel Along Chamber Length

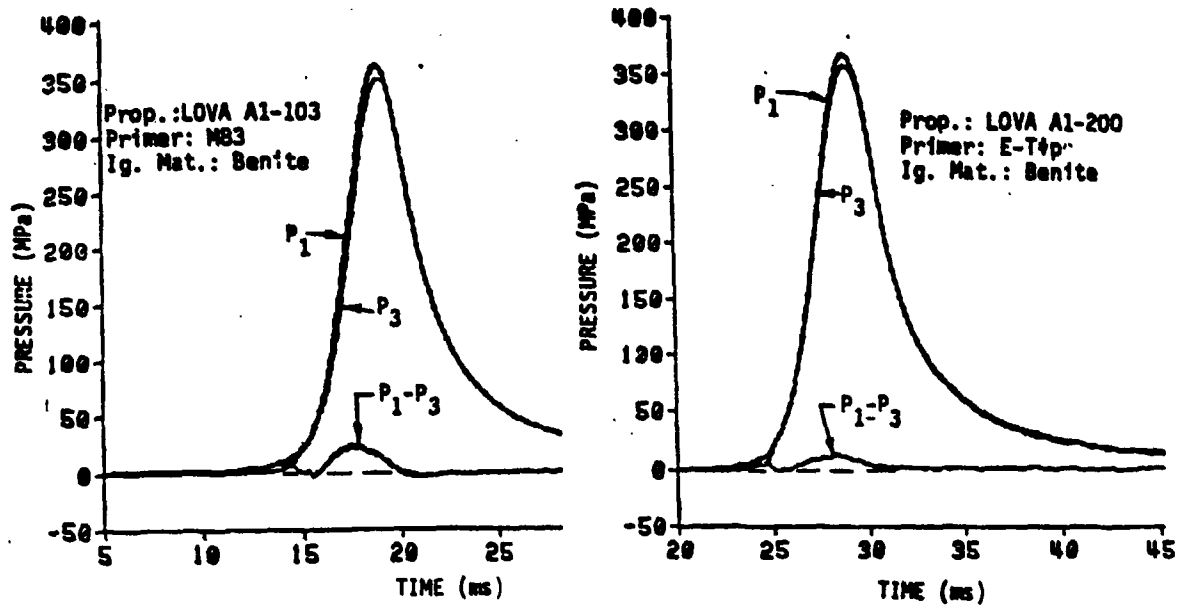


Figure 12. Comparison of Pressure Differences,  $dP$ , Resulting From Gun Firings

Table 2. Ballistic Performance in Gun Firing

ROUND (prop./pri. body /igniter. mat.)	STANDARD DEVIATIONS*			TEMPERATURE COEFFICIENT**		
	br. pr. (MPa)	mus. vel. (m/s)	ig. del. <sup>§</sup> (ms)	br. pr. (MPa)	mus. vel. (m/s)	ig. del. (ms)
LOVA/M83/Benite	17	8	1	-150	-228	16.0
LOVA/E-tip/Benite	6	4	4	-122	-203	15.6
LOVA/EEF/6828 <sup>§§</sup>	4	2	0.2	-205	-153	3.6

\* Based on a three-round sample.

\*\* The temperature coefficient is defined as the change in performance from 294°K (21°C) to 227°K (-46°C).

§ The ignition delay used in the table is defined as the time interval from the instant that firing voltage was applied to the instant that the breech pressure reached 10 MPa.

§§ This group of three rounds was fired with LOVA Lot 1289BL propellant which resulted in a higher level of breech pressure peak than the other two groups which were fired with LOVA Lot Al-200 propellant.

Figures 13a and 14a present two sets of pressure curves, one with a much longer  $t_{ig}$  than the other. The curves in Figure 13a were recorded from a round fired using the standard M83/Benite primer and those in Figure 14a using a primer called EEF/6828 primer. Both shots used the same bimodal CAB/NC/RDX, Lot 1289BL LOVA propellant. The primer body configuration EEF, shown in Figure 15, is essentially a modified version of the M83. It retains the same tube size of the M83 but has more vent holes in the body in addition to adding a 4-hole vented tip to the end of the primer tube. This design allows the igniter gases to vent more uniformly around the primer tube. Meanwhile, the vented tip provides paths for the igniter gases to vent to the forward part of the propellant bed. The igniter material 6828 (component: NC/NG/KClO<sub>4</sub>/EC = 26/17/57/1) is an oxygen-rich material which produces hotter combustion products than benite. Comparison of Figure 13a and Figure 14a reveals that the modified primer EEF/6828 has achieved a significant reduction in ignition delay. This result is also true in gun firing as seen in Table 2.

A short ignition delay implies a fast ignition process, i.e., fast flamespreading. This can be verified by comparing the photographic data exhibits in Figures 13b and 14b. It took 2.75 ms for the round fired with the M83/Benite primer compared to 1.55 ms for the round fired with the EEF/6828 primer from the time that the flame was first seen on the films to the time of rupturing of the chamber. The traces of the flame fronts plotted in Figure 16 shows that the flame front for the round using the EEF/6828 primer was traveling much faster. A fast flamespreading represents a faster ignition process, which results in a fast pressure rise and thus a short ignition delay, as shown in Figure 14a.

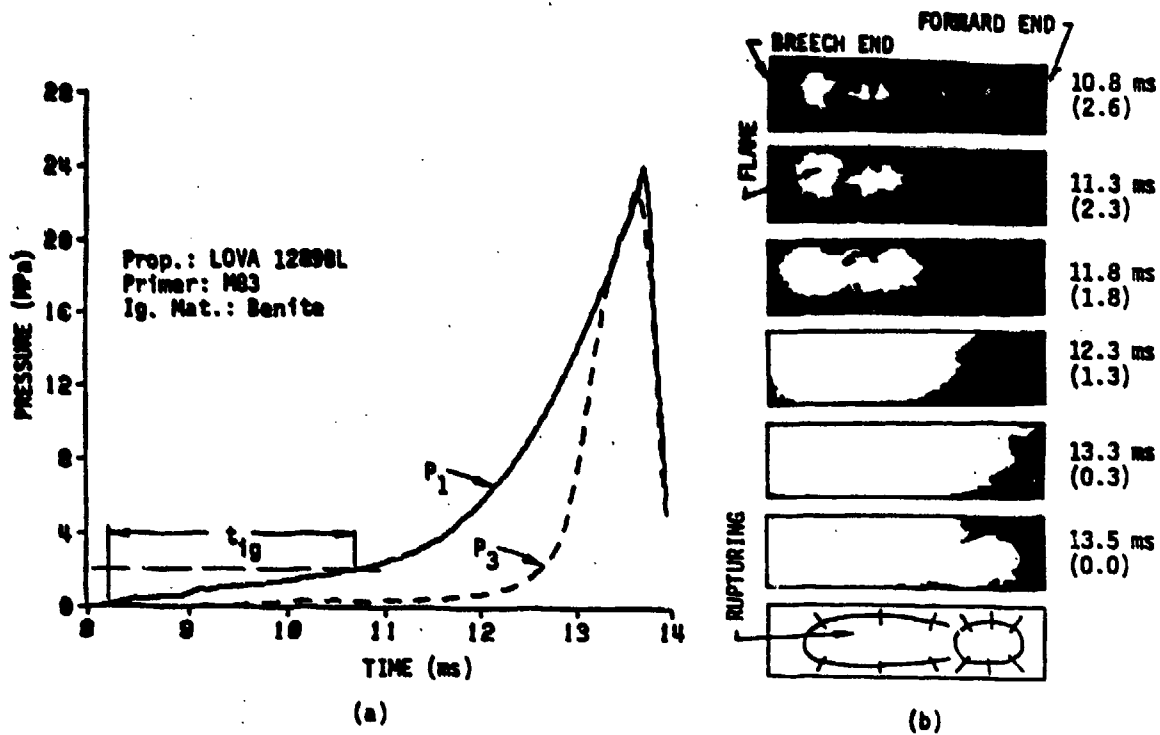


Figure 13. Pressure Rise and Flamespreading, Large  $t_{ig}$

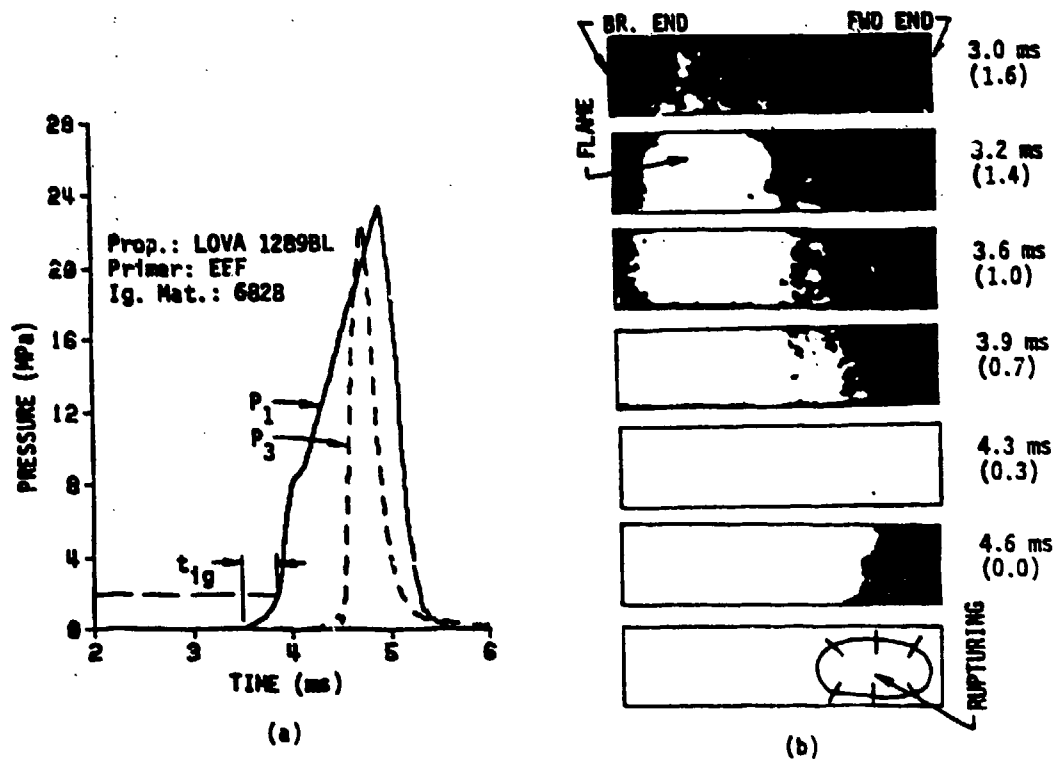


Figure 14. Pressure Rise and Flamespreading, Small  $t_{ig}$

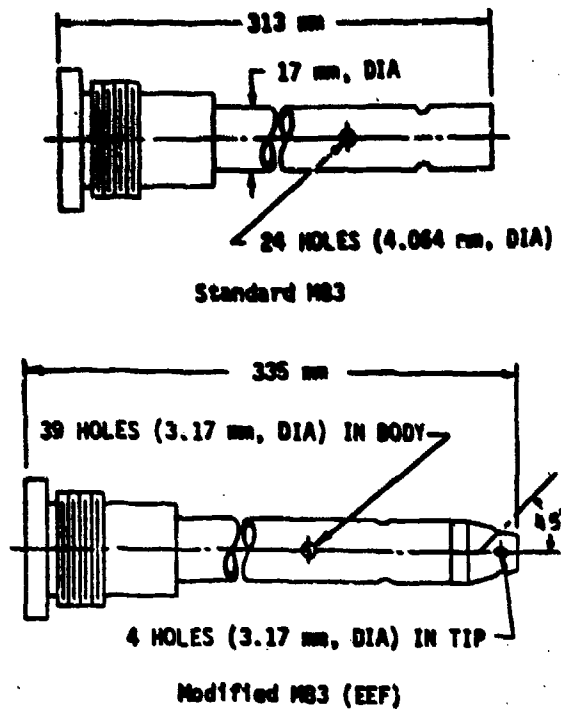


Figure 15. Primer Configurations

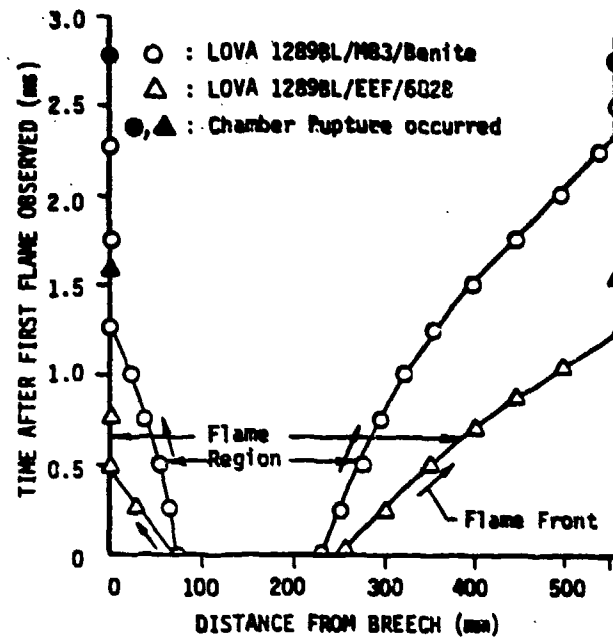


Figure 16. Flame Front Travel Along Chamber Length

Gun firing test data also show a reduction of the ignition delay for the rounds using the EKF/6828 primer, as compared in Figure 17 and Table 2. Indeed, the use of the modified primer has significantly improved the overall ballistic performance, with the exception of the temperature coefficient of the breech pressure.

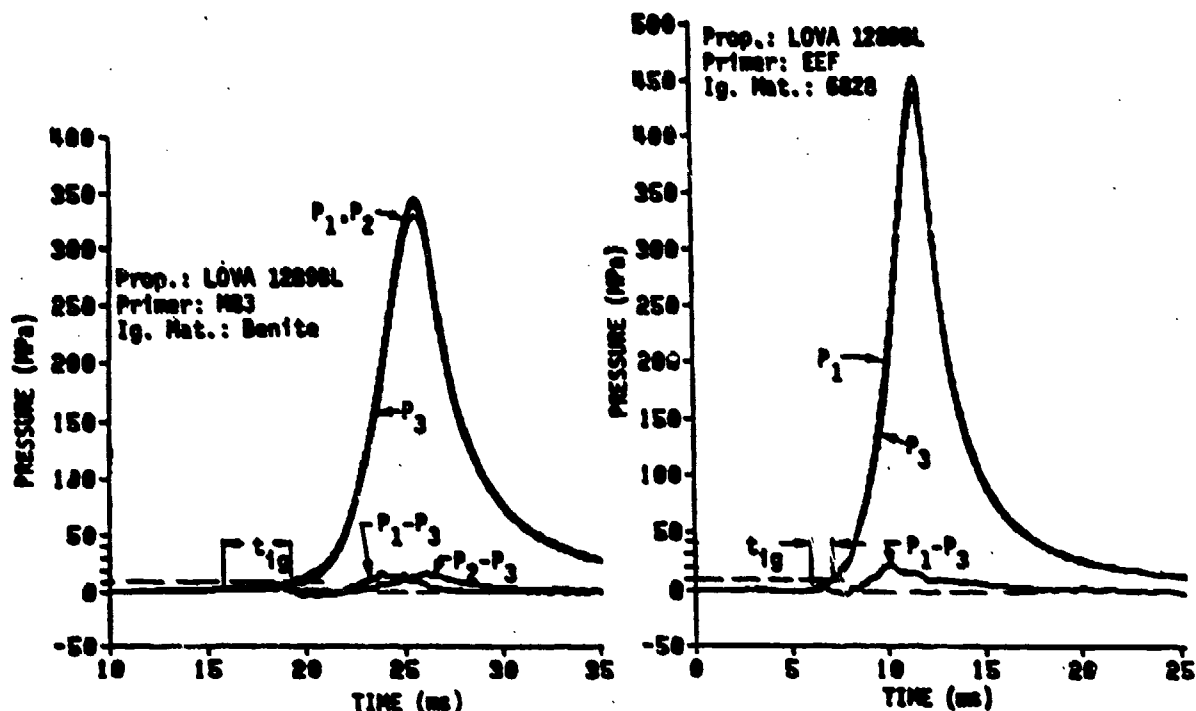


Figure 17. Comparison of Ignition Delays,  $t_{ig}$ , Recorded From Gun Firing Tests

#### E. Effective Ignition of a Propelling Charge

Based on the above discussions, the effectiveness of propellant ignition can be evaluated by examining the ignition delay, pressure data and flamespreading recorded in the simulator diagnostics. To achieve highly effective ignition, the forward end pressure should closely follow the breech pressure and their peak values should occur at the same time. This will ensure a uniform pressure distribution along the propellant bed. The corresponding flamespreading should initiate in a wide range in the central part of the propellant bed and the flame should quickly reach the rear and forward ends of the bed. In addition, the ignition delay should be short, say less than 50 ms to complete the interior ballistic cycle.

#### F. Ullage Effects

Ullage may often appear in a cartridge. It can be caused by the movement of propellant grains during shipment of the ammunition or by the impact occurring during ramming a round into a gun chamber. According to its geometry, ullage may be categorized into three types as depicted in Figure 18. In the first configuration the ullage appears horizontally along the propellant bed. In the second and third configurations the ullage appears in

the corner at the breech end and at the forward end of the chamber, respectively.

The ullage effect for the configuration shown in Figure 18b appearing in a 105-mm advanced kinetic energy cartridge has been investigated by Chang et al.<sup>6</sup> The result shows that an increase in ullage volume increases the ignition delay of the granular LOVA propellant, however, tends to equalize the pressure along the propellant bed at least in the early phase of the interior ballistic cycle. The effect of the ullage shown in Figure 18c has not been published in the open literature to the knowledge of the present author. Nevertheless, in the case that ullage occupied the entire cross-section of the gun chamber at the breech end or at the forward end,<sup>7</sup> its effect on the formation of pressure waves has been found to be strong.

In the following we present the experimental results for two rounds in which the ullage was in the configuration shown in Figure 18a. In the figure the pressure gage  $P_1$  was located right below the ullage while the pressure gage  $P_2$  was way down in the propellant bed. The pressure data obtained are

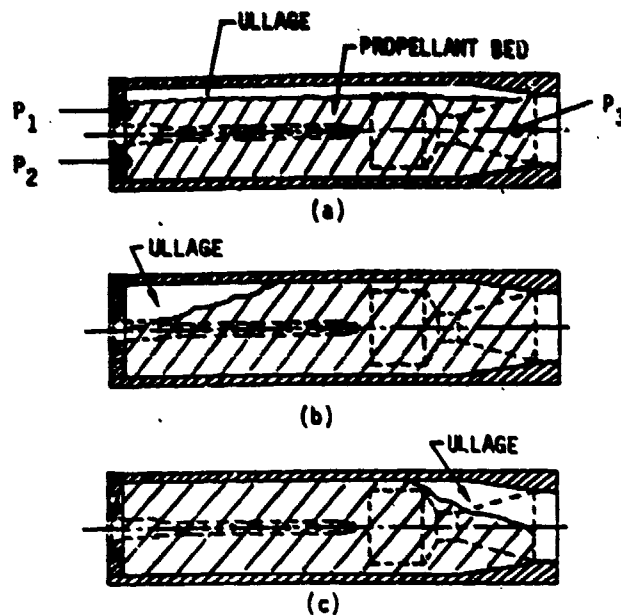


Figure 18. Configurations of Ullage in Propellant Packed Chamber

<sup>6</sup>L.M. Chang, K.P. Resnik, and J.J. Rocchio, "Ignition Studies for Charge Development for an Advanced Kinetic Energy Cartridge," 23rd JANNAF Combustion Meeting, CPIA Publication 457, Vol. II, pp. 307-317, Oct 1986.

<sup>7</sup>Ingo W. May and Albert W. Horst, "Charge Design Considerations and Their Effect on Pressure Waves in Guns," Interior Ballistics of Guns, edited by Herman Krier and Martin Summerfield, Vol. 66, Progress in Astronautics and Aeronautics, Jun 1978.

given in Figure 19a. The lower set of the pressure curves presents only part of the pressure history for the second round due to gage failure. The data in both rounds show that  $P_1$  rose earlier than  $P_2$  by approximately 0.4 ms. The pressure wave initiated by the primer should quickly reach the gage  $P_1$  via the ullage space. Since it needed time to pressurize the ullage volume, the pressure  $P_1$  stayed level for a while before rising again. The pressure  $P_3$  at the forward end of the chamber reached its peak value,  $P_{3p}$ , earlier than  $P_{1p}$ , indicating that the rupture of the chamber occurred earlier in the region near the forward end than in other sections of the chamber.

In chambers without apparent ullage, as those considered early in Sections A through D of this report, we have observed that the flame front advanced to the forward part of the chamber in a pattern nearly normal to the chamber axis. In chambers with ullage as shown in Figures 18a and 18b, however, the advancing pattern is strongly influenced by the geometry of the ullage. For the configuration shown in Figure 18a, the flamespreading is shown in Figure 19b which was reprinted from the high-speed film. On the film we observe that flame (believed largely from the primer at this early period) filled up the entire ullage space above the propellant bed very shortly after its first appearance. Massive propellant ignition then started and the flame

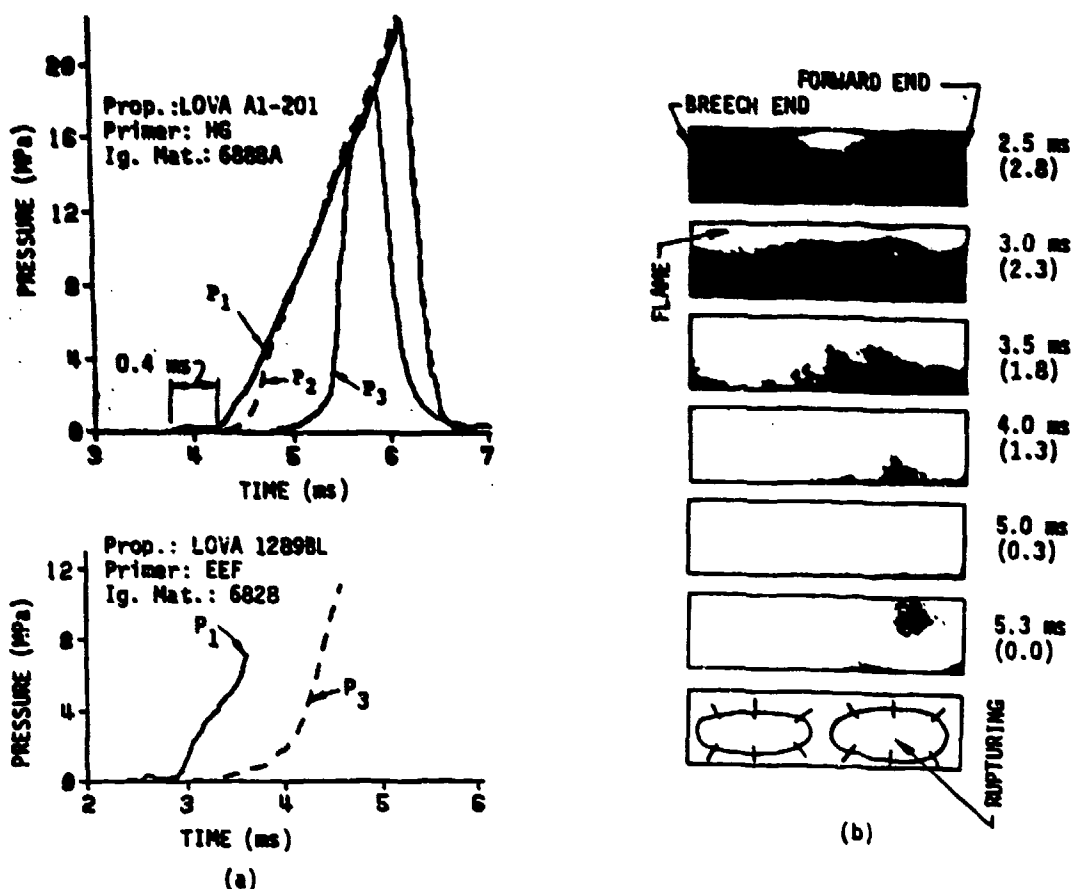


Figure 19. Pressure Rise and Flamespreading in Chambers With Ullage (corresponding to the configuration shown in Figure 18a)

continued to spread to the forward end primarily via the upper part of the propellant bed. After covering the entire stagnation region at the forward end, the flame front headed to the breech end. At this time the propellant bed had three ignition fronts: one adjacent to the ullage and the other two at its two ends. The chamber was completely illuminated before rupturing occurred. The film shows that the rupture initiated near the forward end, which is concurrent with the implication of the pressure data presented above.

#### IV. SUMMARY AND CONCLUSIONS

Close correlations between the pressure and the photographic data have been established based on the pressure histories and the photographic evidence recorded in the simulator diagnostics. With the correlations, the ignition phenomena occurring during the early phase of the interior ballistic cycle can be better understood. Even if only the pressure data are available, the flamespreading in the propellant bed can be visualized.

The breech pressure peak occurred before or after the projectile pressure peak would correspondingly indicate that the high pressure region was located near the breech or near the forward end of the chamber at the time of rupturing of the chamber. When the pressure data show that the high pressure occurred near the breech, the implication is that the flamespreading was slow and it often had not reached the forward part of the chamber by the time of rupturing. In other words, the ignition was localized near the breech. On the other hand, if the high pressure occurred near the forward end, the implication is that the flamespreading was fast and it had covered the entire chamber length at the time of rupturing. That means that the ignition process was very fast and/or an abnormal ignition process was taking place at the forward end of the chamber due to propellant bed compaction or grain fracture.

In the case that the two pressure peaks at the breech and at the forward end occurred at about the same time, there are two possibilities for the pressure distribution along the chamber. One is that a high pressure region was located at the mid section of the chamber and the other is that the pressure distribution was uniform along the chamber. This depends on whether the difference between the two peak pressures is large or small. A small difference implies a uniform pressure distribution. When the pressure distribution was uniform the film shows that the flamespreading was also uniform and had covered the entire chamber length at the time that the chamber ruptured.

To achieve highly effective ignition of a propelling charge, the forward end pressure should closely follow the breech pressure and their peak values should occur at the same time at the instant of chamber rupture. This will ensure a uniform pressure distribution along the propellant bed. The corresponding flamespreading should initiate in a wide range near in the central part of the bed and should quickly reach its rear and forward ends. In addition, the ignition delay should be short, say less than 50 ms to complete the interior ballistic cycle.

Gun firing test data as well as the results of the simulator diagnostics indicate that the use of the modified primers which have a vented tip and more vent holes in a small diameter in the body, namely, M83 with E-tip and EEF, improve the interior ballistic performance of LOVA charges.

Apparent ullage appearing along the top of a propellant bed was found to have a strong influence on the ignition process. Through the ullage space the flame would quickly reach the forward end of the chamber. The ignition of propellant then occurred at three fronts: one in the connection with the ullage and the other two at the two ends of the propellant bed. The flamespreading in the circumferential direction along the chamber in the early period of the ignition process became non-uniform. This might produce an uneven pressure distribution and thus an unbalanced side force acting on the circumference of the projectile afterbody.

## REFERENCES

1. T.C. Minor, "Ignition Phenomena in Combustible-cased Stick Propellant Charges," 19th JANNAF Combustion Meeting, CPIA Publication 366, Vol. I, pp. 555-567, Oct 1982.
2. T.C. Minor, "Experimental Studies of Multidimensional Two-phase Flow Processes in Interior Ballistics," ARBRL-MR-03248; U.S. Army Ballistic Research Laboratory, Apr 1983 (AD A128034).
3. L.M. Chang and J.J. Rocchio, "Early Phase Interior Ballistic Cycle Studies in a Tank Gun Simulator," Proceedings of the 8th International Symposium on Ballistics, pp. I-13 - I-24, Oct 1984.
4. L.M. Chang, "Early Phase Ignition Phenomena Observed in a Tank Gun Chamber, 21st JANNAF Combustion Meeting, CPIA Publication 412, Vol. II, pp. 301-311, Oct 1984.
5. L.M. Chang, "Mechanism of Formation of High-Amplitude Pressure Waves in the 5-In./54 LOVA Charge," 23rd JANNAF Combustion Meeting, CPIA Publication 457, Vol. II, pp. 297-306, Oct 1986.
6. L.M. Chang, K.P. Resnik, and J.J. Rocchio, "Ignition Studies for Charge Development for an Advanced Kinetic Energy Cartridge," 23rd JANNAF Combustion Meeting, CPIA Publication 457, Vol. II, pp. 307-317, Oct 1986.
7. Ingo W. May and Albert W. Horst, "Charge Design Considerations and Their Effect on Pressure Waves in Guns," Interior Ballistics of Guns, edited by Herman Krier and Matrin Summerfield, Vol. 66, Progress in Astronautics and Aeronautics, Jun 1978.

**DISTRIBUTION LIST**

<u>No. Of Copies</u>	<u>Organization</u>	<u>No. Of Copies</u>	<u>Organization</u>
12	Administrator Defense Technical Info Center ATTN: DTIC-DDA Cameron Station Alexandria, VA 22304-6145	5	Project Manager Cannon Artillery Weapons System, ARDEC, AMCCOM ATTN: AMCPM-CW, F. Menke AMCPM-CWW AMCPM-CWS, M. Fisette AMCPM-CWA R. Dekleine H. Hassmann Dover, NJ 07801-5001
1	Commander USA Concepts Analysis Agency ATTN: D. Hardison 8120 Woodmont Avenue Bethesda, MD 20014-2797	20	Commander US Army ARDEC, AMCCOM ATTN: SMCAR-TSS SMCAR-TDC SMCAR-LC LTC N. Barron SMCAR-AEE-BP A. Beardell D. Downs S. Einstein S. Westley S. Bernstein C. Roller J. Rutkowski SMCAR-LCB-I D. Spring SMCAR-LCE SMCAR-LCM-E S. Kaplowitz SMCAR-LCS SMCAR-CCH-T E. Barrieres R. Davitt SMCAR-LCU-CV C. Mandala SMCAR-LCW-A M. Salisbury SMCAR-AEE-BP L. Stiefel B. Brodaman Dover, NJ 07801-5001
1	HQDA/DAMA-ART-M Washington, DC 20310-2500		
1	HQDA/DAMA-CSM Washington, DC 20310-2500		
1	HQDA/SARDA Washington, DC 20310-2500		
1	Commander US Army War College ATTN: Library-FF229 Carlisle Barracks, PA 17013		
1	US Army Ballistic Missile Defense Systems Command Advanced Technology Center P.O. Box 1500 Huntsville, AL 35807-3801		
1	Chairman DOD Explosives Safety Board Room 856-C Hoffman Bldg. 1 2461 Eisenhower Avenue Alexandria, VA 22331-9999		
1	Commander US Army Material Command ATTN: AMCPM-WF 5001 Eisenhower Avenue Alexandria, VA 22331-5001		
1	Commander US Army Material Command ATTN: AMCDRA-ST 5001 Eisenhower Avenue Alexandria, VA 22331-5001	2	Project Manager Munitions Production Base Modernization and Expansion ATTN: AMCPM-PBM, A. Siklosi AMCPM-PBM-E, L. Laibson Dover, NJ 07801-5001

DISTRIBUTION LIST

<u>No. of Copies</u>	<u>Organization</u>	<u>No. of Copies</u>	<u>Organization</u>
3	Project Manager Tank Main Armament System ATTN: AMCPM-TMA, K. Russell AMCPM-TMA-105 AMCPM-TMA-120 Dover, NJ 07801-5001	1	Commander US Army Communications - Electronics Command ATTN: AMSEL-ED Fort Monmouth, NJ 07703-5301
1	Commander US Army Watervliet Arsenal ATTN: SARWV-RD, R. Thierry Watervliet, NY 12189-5001	1	Commander ERADCOM Technical Library ATTN: DELSD-L (Report Section Fort Monmouth, NJ 07703-5301
4	Commander US Army Armament Munitions and Chemical Command ATTN: SMCAR-ESP-L Rock Island, IL 61299-7300	1	Commander US Army Harry Diamond Lab. ATTN: DELHD-TA-L 2800 Powder Mill Road Adelphi, MD 20783-1145
1	HRDA DAMA-ART-M Washington, DC 20310-2500	1	Commander US Army Missile Command ATTN: AMSMI-CM Redstone Arsenal, AL 35898-5249
1	Director Benet Weapons Laboratory Armament Rech Dep & Eng Center US Army AMCCOM ATTN: SMCAR-CCB-TL Watervliet, NY 12189-5001	1	Director US Army Missile and Space Intelligence Center ATTN: AIAMS-YDL Redstone Arsenal, AL 35898-5500
1	Commander US Army Aviation Research and Development Command ATTN: AMSAV-E 4300 Goodfellow Blvd. St. Louis, MO 63120-1702	1	Commander US Army Missile Command Research, Development, and Engineering Center ATTN: AMSMI-RD Redstone Arsenal, AL 35898-5500
1	Commander US Army TSARCOM 4300 Goodfellow Blvd. St. Louis, MO 63120-1702	1	Commander US Army Aviation School ATTN: Aviation Agency Fort Rucker, AL 36360
1	Director US Army Air Mobility Research and Development Laboratory Ames Research Center Moffett Field, CA 94035-1099	1	Commander US Army Tank Automotive Command ATTN: AMSTA-TSL Warren, MI 48092-2498

DISTRIBUTION LIST

<u>No. of Copies</u>	<u>Organization</u>	<u>No. of Copies</u>	<u>Organization</u>
1	Commander US Army Tank Automotive Command ATTN: AMSTA-CG Warren, MI 48092-2498	2	Commander US Army Materials and Mechanics Research Center ATTN: AMKMR-ATL Tech Library Watertown, MA 02172
1	Project Manager Improved TOW Vehicle ATTN: AMCPM-ITV US Army Tank Automotive Command Warren, MI 48092-2498	1	Commander US Army Research Office ATTN: Tech Library P.O. Box 12211 Research Triangle Park, NC 27709-2211
2	Project Manager M1 Abrams Tank Systems ATTN: AMCPM-GMC-SA, T. Dean Warren, MI 48092-2498	1	Commander US Army Belvoir Research & Development Center ATTN: STRBE-WC Fort Belvoir, VA 22060-5606
1	Project Manager Fighting Vehicle Systems ATTN: AMCPM-FVS Warren, MI 48092-2498	1	Commander US Army Logistics Mgmt Ctr Defense Logistics Studies Fort Lee, VA 23801
1	President US Army Armor & Engineer Board ATTN: ATZK-AD-S Fort Knox, KY 40121-5200	1	Commander US Army Infantry School ATTN: ATSH-CD-CSO-OR Fort Benning, GA 31905
1	Project Manager M-60 Tank Development ATTN: AMCPM-M60TD Warren, MI 48092-2498	1	President US Army Artillery Board Ft. Sill, OK 73503-5600
1	Director US Army TRADOC Systems Analysis Activity ATTN: ATAA-SL White Sands Missile Range, NM 88002	1	Commandant US Army Command and General Staff College Fort Leavenworth, KS 66027
1	Commander US Army Training & Doctrine Command ATTN: ATCD-MA/ MAJ Williams Fort Monroe, VA 23651	1	Commandant US Army Special Warfare School ATTN: Rev & Tng Lit Div Fort Bragg, NC 28307
		3	Commander Radford Army Ammunition Plant ATTN: SMCRA-QA/HI LIB Radford, VA 24141-0298

DISTRIBUTION LIST

<u>No. of Copies</u>	<u>Organization</u>	<u>No. of Copies</u>	<u>Organization</u>
1	Commander US Army Foreign Science & Technology Center ATTN: AMXST-MC-3 220 Seventh Street, NE Charlottesville, VA 22901-5396	1	Assistant Secretary of the Navy (R, E, and S) ATTN: R. Reichenbach Room 5E787 Pentagon Bldg. Washington, DC 20350
2	Commandant US Army Field Artillery Center & School ATTN: ATSF-CO-MW, B. Willis Ft. Sill, OK 73503-5600	1	Naval Research Lab Tech Library Washington, DC 20375
1	Commander US Army Development and Employment Agency ATTN: MODE-TED-SAB Fort Lewis, WA 98433-5099	5	Commander Naval Surface Weapons Center ATTN: Code G33 J. L. East W. Burrell J. Johndrow Code G23, D. McClure Code DX-21 Tech Lib Dahlgren, VA 22448-5000
1	Chief of Naval Material Department of Navy ATTN: J. Amlie Arlington, VA 20360	2	Commander US Naval Surface Weapons Center ATTN: J. P. Consaga C. Gotzmer Indian Head, MD 20640-5000
1	Office of Naval Research ATTN: Code 473, R. S. Miller 800 N. Quincy Street Arlington, VA 22217-9999	4	Commander US Naval Surface Weapons Center ATTN: S. Jacobs/Code 240 Code 730 K. Kim/Code R-13 R. Bernecker Silver Springs, MD 20903-5000
3	Commandant US Army Armor School ATTN: ATZK-CD-MS M. Falkovitch Armor Agency Fort Knox, KY 40121-5215	2	Commanding Officer Naval Underwater Systems Center Energy Conversion Dept. ATTN: Code 5B331, R. S. Lazar Tech Lib Newport, RI 02840
2	Commander Naval Sea Systems Command ATTN: SEA 62R SEA 64 Washington, DC 20362-5101		
1	Commander Naval Air Systems Command ATTN: AIR-954-Tech Lib Washington, DC 20360		



**DISTRIBUTION LIST**

<u>No. of Copies</u>	<u>Organisation</u>	<u>No. of Copies</u>	<u>Organisation</u>
10	Central Intelligence Agency Office of Central Reference Dissemination Branch Room GE-47 HQS Washington, DC 20505	2	Director Los Alamos Scientific Lab ATTN: T3, D. Butler M. Division P.O. Box 1663 Los Alamos, NM 87544
1	General Electric Company Armament Systems Dept. ATTN: M. J. Bulman Room 1311 128 Lakeside Avenue Burlington, VT 05401-4985		<u>Aberdeen Proving Ground</u>
1	Hercules Inc. Radford Army Ammunition Plant ATTN: J. Pierce Radford, VA 24141-0299		Dir, USAMSAA ATTN: AMXSY-D AMXSY-MP, H. Cohen
1	Paul Gough Associates, Inc. ATTN: P. S. Gough P.O. Box 1614 1048 South Street Portsmouth, NH 03801-1614		Cdr, USATECOM ATTN: AMSTE-TO-F AMSTE-CM-F, L. Nealley
1	Princeton Combustion research Lab., Inc. ATTN: M. Summerfield 475 US Highway One Monmouth Junction, NJ 08852-9650		Cdr, CSTA ATTN: STECS-AS-H, R. Hendricksen
1	Battelle Memorial Institute ATTN: Tech Library 505 King Avenue Columbus, OH 43201-2693		Cdr, CRDEC, AMCCOM ATTN: SMCCR-RSP-A SMCCR-MU SMCCR-SPS-IL
1	Johns Hopkins University Applied Physics Laboratory Chemical Propulsion Information Agency ATTN: T. Christian Johns Hopkins Road Laurel, MD 20707-0690		
1	Pennsylvania State University Dept. of Mech. Engineering ATTN: K. Kuo University Park, PA 16802-7501		

USER EVALUATION SHEET/CHANGE OF ADDRESS

This Laboratory undertakes a continuing effort to improve the quality of the reports it publishes. Your comments/answers to the items/questions below will aid us in our efforts.

1. BRL Report Number \_\_\_\_\_ Date of Report \_\_\_\_\_

2. Date Report Received \_\_\_\_\_

3. Does this report satisfy a need? (Comment on purpose, related project, or other area of interest for which the report will be used.) \_\_\_\_\_

4. How specifically, is the report being used? (Information source, design data, procedure, source of ideas, etc.) \_\_\_\_\_

5. Has the information in this report led to any quantitative savings as far as man-hours or dollars saved, operating costs avoided or efficiencies achieved, etc? If so, please elaborate. \_\_\_\_\_

6. General Comments. What do you think should be changed to improve future reports? (Indicate changes to organization, technical content, format, etc.) \_\_\_\_\_

CURRENT ADDRESS

Name \_\_\_\_\_

Organization \_\_\_\_\_

Address \_\_\_\_\_

City, State, Zip \_\_\_\_\_

7. If indicating a Change of Address or Address Correction, please provide the New or Correct Address in Block 6 above and the Old or Incorrect address below.

OLD ADDRESS

Name \_\_\_\_\_

Organization \_\_\_\_\_

Address \_\_\_\_\_

City, State, Zip \_\_\_\_\_

(Remove this sheet, fold as indicated, staple or tape closed, and mail.)